LETTER

doi:10.1038/nature09477

Hidden magnetic excitation in the pseudogap phase of a high-T_c superconductor

Yuan Li[1]†, V. Balédent[2], G. Yu[3], N. Barišić[4,5]†, K. Hradil[6], R. A. Mole[7], Y. Sidis[2], P. Steffens[8], X. Zhao[4,9], P. Bourges[2] & M. Greven[3]

The elucidation of the pseudogap phenomenon of the high-transition-temperature (high-T_c) copper oxides—a set of anomalous physical properties below the characteristic temperature T^* and above T_c—has been a major challenge in condensed matter physics for the past two decades[1]. Following initial indications of broken time-reversal symmetry in photoemission experiments[2], recent polarized neutron diffraction work demonstrated the universal existence of an unusual magnetic order below T^* (refs 3, 4). These findings have the profound implication that the pseudogap regime constitutes a genuine new phase of matter rather than a mere crossover phenomenon. They are furthermore consistent with a particular type of order involving circulating orbital currents, and with the notion that the phase diagram is controlled by a quantum critical point[5]. Here we report inelastic neutron scattering results for $HgBa_2CuO_{4+\delta}$ that reveal a fundamental collective magnetic mode associated with the unusual order, and which further support this picture. The mode's intensity rises below the same temperature T^* and its dispersion is weak, as expected for an Ising-like order parameter[6]. Its energy of 52–56 meV renders it a new candidate for the hitherto unexplained ubiquitous electron–boson coupling features observed in spectroscopic studies[7–10].

Our measurements were performed on three samples made of co-aligned crystals, which were grown by a self-flux method[11] and were free from substantial macroscopic impurity phases and inhomogeneity (Supplementary Information sections 1 and 2). $HgBa_2CuO_{4+\delta}$ (Hg1201) exhibits the highest value of T_c of all copper oxides with one copper–oxygen plane per unit cell, has a simple tetragonal structure, and is furthermore thought to be relatively free of disorder effects[12,13]. Here we quote the scattering wave vector as $\mathbf{Q} = H\mathbf{a}^* + K\mathbf{b}^* + L\mathbf{c}^* \equiv (H,K,L)$ in reciprocal lattice units (r.l.u.), where $\mathbf{a}^*$, $\mathbf{b}^*$ and $\mathbf{c}^*$ are reciprocal lattice vectors. We present normalized neutron intensities in most figures to facilitate a direct comparison of the intensity among the measurements (the normalization process is described in Supplementary Information section 3).

Spin-polarized inelastic neutron scattering data (Fig. 1) demonstrate the existence of a magnetic excitation throughout the two-dimensional (2D) Brillouin zone in a nearly optimally doped sample ($T_c = 94.5 \pm 2$ K, denoted OP95). Energy scans in the spin-flip channel reveal a resolution-limited feature at low temperatures, with a weak dispersion and a maximum of 56 meV at the 2D zone-corner ($H = K = 0.5$, also referred to as the antiferromagnetic wave vector, $\mathbf{q}_{AF}$). The feature cannot be due to a polarization leakage from the non-spin-flip channel (Supplementary Information section 4), and it disappears in the spin-flip channel at 300 K (Fig. 1a). Background intensity at 10 K has been measured separately using a combination of different spin-polarization geometries (Supplementary Information section 1) and agrees with the intensity at 300 K within the error (Fig. 1a; $H = K = 0.2$). These results prove the magnetic origin of the peak at 10 K.

The dispersion of the excitation along (H, H) for both this optimally doped sample and an underdoped sample ($T_c = 65 \pm 3$ K, UD65; Supplementary Information section 5), measured with both polarized and unpolarized neutrons, is displayed in Fig. 1c. The weak dispersion

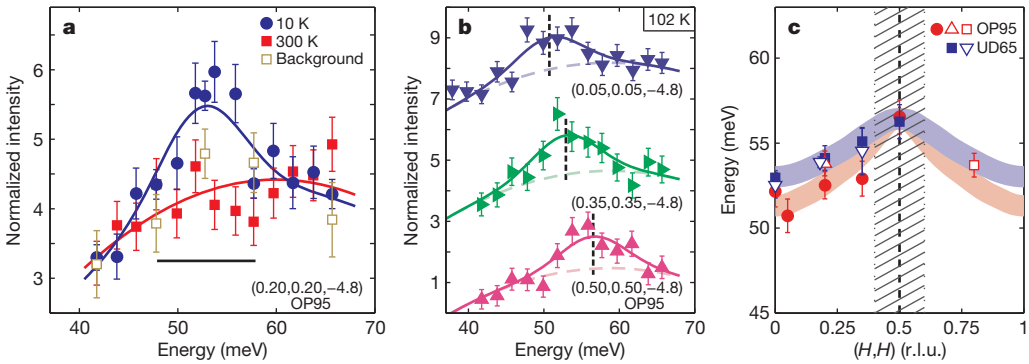

Figure 1 | Identification of a weakly dispersing magnetic collective mode. **a**, Spin-flip energy scans for sample OP95; **Q**-position given at bottom right. Background (open squares) is measured at 10 K by a method described in Supplementary Information section 1 and approximated together with the data at 300 K by a parabolic baseline (red line). The 10 K data are fitted to a Gaussian (blue line) on this baseline, with a small offset to account for the possible background change with temperature. Similar baselines are used in **b** and Fig. 2a. Horizontal bar indicates instrument energy resolution of ~10 meV (FWHM). **b**, Spin-flip energy scans at additional **Q**-positions, offset for clarity. **c**, Summary of dispersion along (H,H). Different symbols represent measurements using different spectrometers: IN20 (circles), PUMA (squares), 2T (triangle) and IN8 (reversed triangle). The measurement on spectrometer IN20 is spin-polarized; all others are unpolarized. Data are presented in panels **a** and **b**, Fig. 2c and d, and Supplementary Figs 4–6. Conventional magnetic response near $\mathbf{q}_{AF}$ (vertical dashed line) is expected in the hatched area (estimated on the basis of Supplementary Fig. 8b–d), where the determination of the dispersion using energy scans may be less accurate. Error bars represent statistical and fit uncertainties (1 s.d.).

[1]Department of Physics, Stanford University, Stanford, California 94305, USA. [2]Laboratoire Léon Brillouin, CEA-CNRS, CEA-Saclay, 91191 Gif sur Yvette, France. [3]School of Physics and Astronomy, University of Minnesota, Minneapolis, Minnesota 55455, USA. [4]T.H. Geballe Laboratory for Advanced Materials, Stanford University, Stanford, California 94305, USA. [5]1. Physikalisches Institut, Universität Stuttgart, 70550 Stuttgart, Germany. [6]Institut für Physikalische Chemie, Universität Göttingen, 37077 Göttingen, Germany. [7]Forschungsneutronenquelle Heinz Maier-Leibnitz, 85747 Garching, Germany. [8]Institut Laue Langevin, 38042 Grenoble Cedex 9, France. [9]State Key Laboratory of Inorganic Synthesis and Preparative Chemistry, College of Chemistry, Jilin University, Changchun 130012, China. †Present addresses: Max Planck Institute for Solid State Research, 70569 Stuttgart, Germany (Y.L.); Institute of Physics, Bijenicka cesta 46, 10 000 Zagreb, Croatia (N.B.).

(<10%) and the strong response at the 2D zone centre $q = 0$ differ drastically from the characteristics of the well-known antiferromagnetic response near $\mathbf{q}_{AF}$ (refs 14, 15). Remarkably, the dispersion of the excitation, which is already present well above T_c, reaches its maximum at the same point in energy–momentum space as the so-called magnetic resonance[16], which in OP95 occurs only below T_c (ref. 17). This is further demonstrated in Fig. 2a: compared to the measurement above T_c, substantially higher intensity is observed at $\mathbf{q}_{AF}$ below T_c.

We emphasize that the magnetic signal far away from $\mathbf{q}_{AF}$ cannot be attributed to a resonance peak that is broad in momentum, for the following reasons. First, at optimal doping, the temperature dependence of the signal away from $\mathbf{q}_{AF}$ (Fig. 3a) is different from that of the resonance[17] (Fig. 2a inset). Second, the excitation energy near $q = 0$ differs from that at $\mathbf{q}_{AF}$ (Fig. 1, Supplementary Fig. 4). Third, the profile of momentum scans at the resonance energy is not symmetric about $\mathbf{q}_{AF}$, but is better described by a broad peak centred at $q = 0$ plus a narrower peak centred at $\mathbf{q}_{AF}$ (Supplementary Fig. 8a). Fourth, the resonance peak in momentum scans does not extend below $H = K = 0.3$ (Supplementary Fig. 8b–d). Therefore, a magnetic excitation branch in addition to the resonance is required to describe the data, as illustrated in Fig. 1c. This excitation branch is also distinctly different from the well-known 'hourglass' excitations[18,19]: the latter only exist in a limited momentum range near $\mathbf{q}_{AF}$ (the hatched area in Fig. 1c) and only become clearly incommensurate[15] below T_c in $YBa_2Cu_3O_{6+\delta}$ (YBCO), whereas the former is observed all the way to $q = 0$ and above T_c (Fig. 1b and Fig. 3). Moreover, following the notion that the hourglass excitations are collective modes below the electron–hole continuum, they are expected only near $\mathbf{q}_{AF}$ and cannot continuously disperse to $q = 0$ (ref. 19).

After the magnetic nature of the excitation was verified with polarized neutrons, further quantitative measurements were carried out with unpolarized neutrons to benefit from the much higher neutron flux. Following standard procedure to extract a magnetic signal[19], phonons and spurious contributions were either removed by subtracting background obtained at high temperature, or avoided by carefully choosing the measurement conditions (Supplementary Information sections 5 and 6). Measurements at 2D **Q**-positions similar to those in Fig. 1a, b, shown in Supplementary Figs 4–6, confirm and extend the spin-polarized results. The excitation was also observed at $\mathbf{q} = (0.5,0)$ (Fig. 2b) and $\mathbf{q} = (0,0.5)$ (Fig. 2c), which are equivalent 2D **Q**-positions rotated 45° away from those summarized in Fig. 1c. The energy width of the excitation was found to remain resolution-limited when measured with better energy resolution (Fig. 2d), which indicates that it is a long-lived mode. As the excitation is observed at all of those **Q**-positions summarized in Fig. 2d inset, we conclude that it is present throughout the entire 2D Brillouin zone.

The temperature dependence of the excitation is best measured away from $\mathbf{q}_{AF}$ and with unpolarized neutrons (Supplementary Information section 6). The results are summarized in Fig. 3a. The onset temperature of the excitation, T_{ex}, is shown in Fig. 3b together with T^* determined from in-plane resistivity[12,20] (Supplementary Information section 7) and the onset temperature of the $q = 0$ magnetic order measured by polarized-neutron diffraction[4]. The good agreement among these results suggests that the excitation is a fundamental collective mode of the universal $q = 0$ pseudogap order[3,4]. As the high-T_c copper oxides are not ferromagnetic, a 'decoration' of the unit cell with a net cancellation of moments is required to account for the observed behaviour. Consequently, the collective mode can not be understood with conventional t-J and one-band Hubbard models[21], which reduce the problem to one site per unit cell, and instead an extended multi-band approach appears necessary[5,22,23].

The unusual phase diagram of the copper oxides has been argued to be controlled by an underlying quantum critical point that marks the termination of a distinct order[5,24–26]. A leading candidate is the $q = 0$

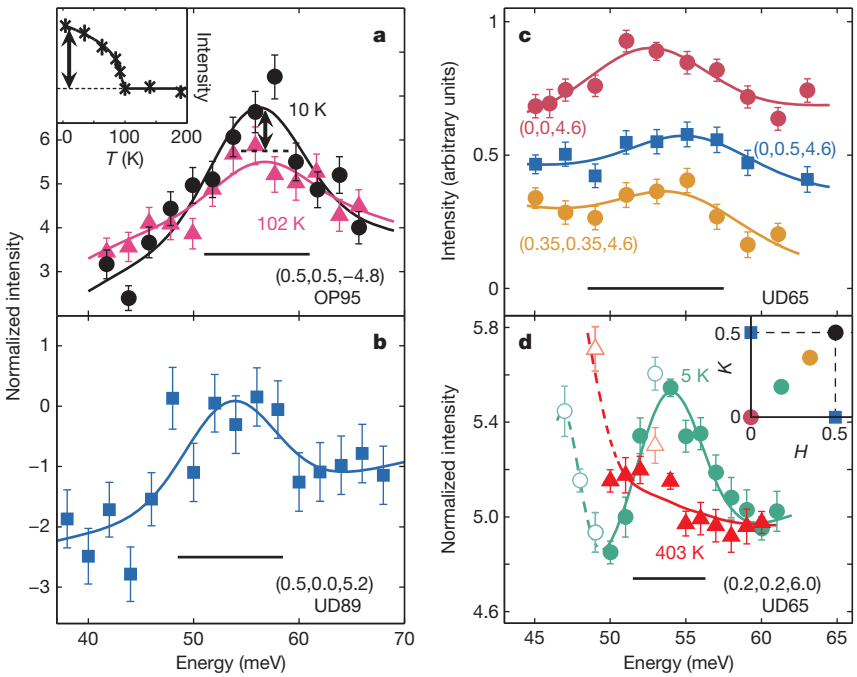

Figure 2 | Presence of the collective mode throughout the entire 2D Brillouin zone. **a**, Spin-flip energy scans at $\mathbf{q}_{AF}$ below and above T_c. Arrow and dashed line indicate the estimated intensity change due to the resonance. The inset is adapted from ref. 17 and illustrates the intensity change of the resonance below T_c. **b**, Unpolarized spectral difference between 16 K and 200 K for sample UD89 ($T_c = 89 \pm 3$ K) at a **Q**-position away from the 2D zone diagonal. **c**, Unpolarized spectral difference between 4 K and 330 K for sample UD65 at three different **Q**-positions in the first 2D Brillouin zone. **d**, Unpolarized measurement for sample UD65 using better energy resolution. A constant has been subtracted from the 403 K data for better comparison. The peak at 5 K is no longer present at 403 K, which is well above T^*. Lines in all panels are Gaussian fits, which serve as guides to the eye. Open symbols in **d** indicate measurement points that seem contaminated by phonons (below 50 meV) and a spurious contribution (at 53 meV). Inset in **d** summarizes the **Q**-positions (colour-coded for the main panels) at which the measurements were performed. Horizontal bars indicate energy resolutions of the instruments (FWHM) and error bars represent statistical uncertainty (1 s.d.).

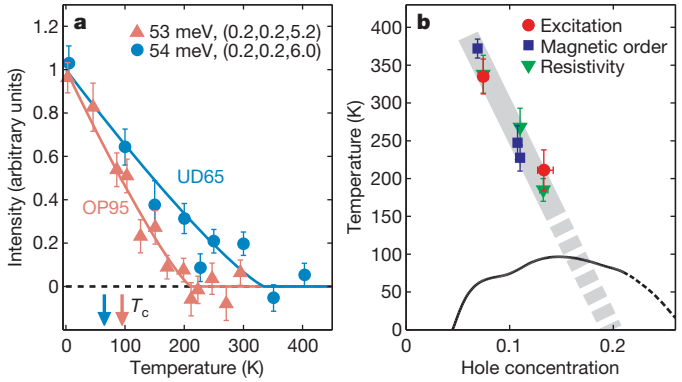

Figure 3 | Temperature dependence of the collective mode demonstrates its connection to the pseudogap phenomenon. **a**, Temperature dependence of intensity measured at 53 meV, $\mathbf{Q} = (0.2,0.2,5.2)$, for sample OP95 (triangles) and at 54 meV, $\mathbf{Q} = (0.2,0.2,6.0)$, for sample UD65 (circles), after background subtraction (Supplementary Information section 6) and normalization to values at the lowest temperature. Lines are empirical power-law fits (Supplementary Information section 6). The onset temperature T_{ex} is 211 ± 13 K near optimal doping and becomes considerably higher (335 ± 23 K) at the lower doping, with no abrupt change near T_c in either case. **b**, Summary of characteristic (onset) temperatures. Red circles, excitation branch (this work); blue squares, $q = 0$ magnetic order[4]; green triangles, in-plane resistivity deviation (refs 12, 20 and Supplementary Information section 7). Hole concentrations are determined after ref. 29 based on the doping dependence of T_c in Hg1201 (black line). Error bars, 1 s.d.

magnetic order that preserves the translational symmetry of the lattice[3,4] and which would naturally give rise to excitations centred at $q = 0$. Indeed, such an ordered state involving circulating charge currents has been predicted theoretically[5,27]. On the basis that this current-loop order is describable by an Ising-like Ashkin-Teller model, a rather unusual magnetic excitation spectrum with nearly dispersion-free excitations is expected from the discrete symmetry of the order parameter[6], consistent with our findings.

In the copper oxides, anomalies in the charge excitation spectrum are usually discussed in terms of a coupling between electrons and bosonic modes (phonons or antiferromagnetic spin fluctuations). The hitherto unobserved excitation found here at the same energy as the resonance, but up to higher temperature and all the way to $q = 0$, is a new candidate for the mysterious electron–boson interaction features observed by photoemission[7], optical spectroscopy[8,9] and scanning tunnelling spectroscopy[10]. At $\mathbf{q}_{AF}$, the strength of the excitation is comparable to that of the resonance (in Hg1201 (Fig. 2a) and YBCO[19]). Whereas the latter is located at $\mathbf{q}_{AF}$, the former extends throughout the entire Brillouin zone (Fig. 2). As the area of resolution ellipsoid in 2D momentum space is a few per cent of the Brillouin zone, we estimate that the momentum-integrated spectral weight of the excitation branch is at least an order of magnitude greater than that of the resonance in Hg1201, and comparable to that of the full antiferromagnetic response in underdoped YBCO (the integrated spectral weight between 25 and 100 meV is believed to be several times larger than that of the resonance[15,28]). In other words, about half of the total magnetic spectral weight is located within a narrow range around the resonance energy, and has been hidden so far, in part due to the excitation's weak momentum dependence. It remains an open question whether the coincidence of energy scales of the excitation and resonance is accidental, or if there is a profound physical connection. Recently, we observed indications of the existence of a second branch of similar excitations at lower energy, which needs to be verified by further studies.

All the evidence[12,13] suggests that Hg1201 is not only representative of the copper oxides, but is a model compound, and therefore experiments on Hg1201 can be expected to reveal the essence of the underlying physics most clearly. Given the universal existence among the copper oxides of the pseudogap phase, of the $q = 0$ magnetic order, and of the electron–boson coupling features in the 50–60 meV range, we expect the excitation branch to be present in other copper oxides as well (Supplementary Information section 9).

Received 12 May; accepted 7 September 2010.

1. Norman, M. R., Pines, D. & Kallin, C. The pseudogap: friend or foe of high T_c? *Adv. Phys.* **54,** 715–733 (2005).
2. Kaminski, A. *et al.* Spontaneous breaking of time-reversal symmetry in the pseudogap state of a high-T_c superconductor. *Nature* **416,** 610–613 (2002).
3. Fauqué, B. *et al.* Magnetic order in the pseudogap phase of high-T_c superconductors. *Phys. Rev. Lett.* **96,** 197001 (2006).
4. Li, Y. *et al.* Unusual magnetic order in the pseudogap region of the superconductor $HgBa_2CuO_{4+\delta}$. *Nature* **455,** 372–375 (2008).
5. Varma, C. M. Non-Fermi-liquid states and pairing instability of a general model of copper oxide metals. *Phys. Rev. B* **55,** 14554–14580 (1997).
6. Varma, C. M. Theory of the pseudogap state of the cuprates. *Phys. Rev. B* **73,** 155113 (2006).
7. Lanzara, A. *et al.* Evidence for ubiquitous strong electron-phonon coupling in high-temperature superconductors. *Nature* **412,** 510–514 (2001).
8. Yang, J. *et al.* Exchange boson dynamics in cuprates: optical conductivity of $HgBa_2CuO_{4+\delta}$. *Phys. Rev. Lett.* **102,** 027003 (2009).
9. van Heumen, E. *et al.* Optical determination of the relation between the electron-boson coupling function and the critical temperature in high-T_c cuprates. *Phys. Rev. B* **79,** 184512 (2009).
10. Lee, J. *et al.* Interplay of electron-lattice interactions and superconductivity in $Bi_2Sr_2CaCu_2O_{8+\delta}$. *Nature* **442,** 546–550 (2006).
11. Zhao, X. *et al.* Crystal growth and characterization of the model high-temperature superconductor $HgBa_2CuO_{4+\delta}$. *Adv. Mater.* **18,** 3243–3247 (2006).
12. Barišić, N. *et al.* Demonstrating the model nature of the high-temperature superconductor $HgBa_2CuO_{4+\delta}$. *Phys. Rev. B* **78,** 054518 (2008).
13. Eisaki, H. *et al.* Effect of chemical inhomogeneity in bismuth-based copper oxide superconductors. *Phys. Rev. B* **69,** 064512 (2004).
14. Vignolle, B. *et al.* Two energy scales in the spin excitations of the high-temperature superconductor $La_{2-x}Sr_xCuO_4$. *Nature Phys.* **3,** 163–167 (2007).
15. Hinkov, V. *et al.* Spin dynamics in the pseudogap state of a high-temperature superconductor. *Nature Phys.* **3,** 780–785 (2007).
16. Rossat-Mignod, J. *et al.* Neutron scattering study of the $YBa_2Cu_3O_{6+x}$ system. *Physica C* **185–189,** 86–92 (1991).
17. Yu, G. *et al.* Magnetic resonance in the model high-temperature superconductor $HgBa_2CuO_{4+\delta}$. *Phys. Rev. B* **81,** 064518 (2010).
18. Tranquada, J. M. *et al.* Quantum magnetic excitations from stripes in copper oxide superconductors. *Nature* **429,** 534–538 (2004).
19. Pailhès, S. *et al.* Resonant magnetic excitations at high energy in superconducting $YBa_2Cu_3O_{6.85}$. *Phys. Rev. Lett.* **93,** 167001 (2004).
20. Grbić, M. S. *et al.* Microwave measurements of the in-plane and *c*-axis conductivity in $HgBa_2CuO_{4+\delta}$: discriminating between superconducting fluctuations and pseudogap effects. *Phys. Rev. B* **80,** 094511 (2009).
21. Norman, M. R. & Pépin, C. The electronic nature of high temperature cuprate superconductors. *Rep. Prog. Phys.* **66,** 1547–1610 (2003).
22. Tahir-Kheli, J. & Goddard, W. A. III. Chiral plaquette polaron theory of cuprate superconductivity. *Phys. Rev. B* **76,** 014514 (2007).
23. Weber, C. *et al.* Orbital currents in extended Hubbard models of high-T_c cuprate superconductors. *Phys. Rev. Lett.* **102,** 017005 (2009).
24. Kivelson, S. A., Fradkin, E. & Emery, V. J. Electronic liquid-crystal phases of a doped Mott insulator. *Nature* **393,** 550–553 (1998).
25. Sachdev, S. Quantum criticality: competing ground states in low dimensions. *Science* **288,** 475–480 (2000).
26. Chakravarty, S. *et al.* Hidden order in the cuprates. *Phys. Rev. B* **63,** 094503 (2001).
27. Simon, M. E. & Varma, C. M. Detection and implications of a time-reversal breaking state in underdoped cuprates. *Phys. Rev. Lett.* **89,** 247003 (2002).
28. Hayden, S. M. *et al.* The structure of the high-energy spin excitations in a high-transition-temperature superconductor. *Nature* **429,** 531–534 (2004).
29. Yamamoto, A., Hu, W. & Tajima, S. Thermoelectric power and resistivity of $HgBa_2CuO_{4+\delta}$ over a wide doping range. *Phys. Rev. B* **63,** 024504 (2000).

Supplementary Information is linked to the online version of the paper at www.nature.com/nature.

Acknowledgements We thank T. H. Geballe, S. A. Kivelson, E. M. Motoyama and C. M. Varma for discussions. This work was supported by the US Department of Energy and the US National Science Foundation, and by the National Natural Science Foundation, China. Y.L. acknowledges support from the Alexander von Humboldt Foundation during the final stage of completing the manuscript.

Author Contributions M.G., P.B. and Y.L. planned the project. Y.L., V.B. and G.Y. performed the neutron scattering experiments. Y.L., N.B. and X.Z. characterized and prepared the samples. N.B. performed the resistivity measurements. P.S., R.A.M., K.H., Y.S. and P.B. were local contacts for the neutron scattering experiments. Y.L. and M.G. analysed the data and wrote the manuscript.

Author Information Reprints and permissions information is available at www.nature.com/reprints. The authors declare no competing financial interests. Readers are welcome to comment on the online version of this article at www.nature.com/nature. Correspondence and requests for materials should be addressed to M.G. (greven@physics.umn.edu).